

## Comprehensive bioinformatics analysis of key miRNAs and signaling pathways in the body fluids of human knee osteoarthritis

Mahshid Malakootian<sup>1#</sup>, Akram Gholipour<sup>1#</sup>, Maziar Oveisee<sup>2\*</sup><sup>1</sup>Cardiogenetics Research Center, Rajaie Cardiovascular Medical and Research Center, Iran University of Medical Sciences, Tehran, Iran<sup>2</sup>Orthopedic Department, School of Medicine, Bam University of Medical Sciences, Bam, Iran

#These authors have contributed equally to this work.

### ARTICLE INFO

#### Original paper

#### Article history:

Received: July 03, 2023

Accepted: October 15, 2023

Published: November 30, 2023

#### Keywords:

Osteoarthritis, Overlapping miRNAs, Signaling pathways

### ABSTRACT

Osteoarthritis (OA) is one of the principal causes of chronic joint disease with a series of pathological features. The present study aimed to identify key microRNAs (miRNAs) and signaling pathways in OA biological fluids to explain the potential mechanisms underlying the disease and introduce OA biomarkers using computational analysis. Differentially expressed microRNAs (DEmiRNAs) in the serum, plasma, and synovial fluids of OA patients were identified using the GEO2R, limma, and DESeq2 packages in the R software based on the dataset from GSE151341, GSE105027, and GSE126677. The gene ontology (GO) enrichment, Kyoto Encyclopedia of Genes and Genomes (KEGG), and network construction analyses were performed for overlapping DEmiRNAs. Forty DEmiRNAs overlapped in the plasma, serum, and synovial fluids of OA patients. The expression patterns of the DEmiRNAs in the serum and plasma were almost the same, while they were reversed in the synovial fluid. Differentially expressed hsa-miR-146a-5p and hsa-miR-335-5p miRNAs showed downregulation in all 3 OA sample types. According to enrichment analysis regarding OA pathogenesis, the signaling pathways of TGF- $\beta$ , Hippo, FoxO, PI3K-Akt, and mTOR were significant, with hsa-miR-146a-5p and hsa-miR-335-5p involved in their regulation. The present informatics study for the first time provides insights into the potential diagnostic targets of OA by analyzing overlapping miRNAs and their relevant signaling pathways in human knee fluids (serum, plasma, and synovial fluids).

Doi: <http://dx.doi.org/10.14715/cmb/2023.69.12.15>Copyright: © 2023 by the C.M.B. Association. All rights reserved. 

### Introduction

Osteoarthritis (OA) is a degenerative joint disease whose incidence is on the rise in the elderly (1). The pathological features of OA comprise articular cartilage degradation, synovial inflammation, subchondral bone sclerosis, and osteophyte development (2, 3). This chronic joint pain and its associated disability are acknowledged as the principal source of socioeconomic burdens on healthcare systems (4, 5).

The current diagnostic and treatment approaches to OA, applied to all patients, chiefly seek to ameliorate symptomatic pains or substitute joint surgery in severe conditions (6). To our knowledge, no pharmaceutical agents exist to lessen or stop OA progression (7). Nonetheless, novel therapeutic approaches, including autologous chondrocyte implantation and matrix-based autologous chondrocyte implantation, can improve 80% of symptoms, with changeable efficacies in various individuals (8).

The paucity of diagnostic and treatment strategies and limited knowledge concerning the exact pathological mechanisms underlying OA underscore the necessity of molecular research on the mechanisms involved.

To date, the rapid development of transcriptome and gene-expression high-throughput technologies, such as

microarray and next-generation sequencing analyses, in tandem with clinical information, has helped clarify the mechanisms involved in OA pathogenesis and predict the efficacy of the treatment (9, 10). Transcriptome profiling is a quantitative measurement of RNA levels (coding and noncoding) for thousands of genes simultaneously, manufacturing a broad picture of cellular function and contributing to personalized medicine.

Nowadays, human body fluids are deemed appealing sources for clinical biomarkers since their collection and processing are less invasive, less costly, and more rapid (11, 12). In addition, the altered expression profiles of messenger RNAs (mRNAs), long noncoding RNAs (lncRNAs), and microRNAs (miRNAs) may reflect the cellular mechanisms underlying the pathological states (11). Accordingly, screening human body fluids is one of the most promising approaches to discern biomarkers or unveil pathophysiological mechanisms for human disorders.

The present study aimed to provide a comprehensive understanding of miRNA expression alterations in the serum, plasma, and synovial fluids of patients with OA and introduce potential miRNAs as noninvasive OA biomarkers.

\* Corresponding author. Email: [dr.oveisee.m@gmail.com](mailto:dr.oveisee.m@gmail.com)

## Materials and Methods

### The expression profiles of miRNAs in the body fluids of human knee OA

First, miRNA profiling in knee OA plasma, chondrocyte serum, and synovial fluid samples was obtained from the Gene Expression Omnibus (GEO) datasets GSE151341, GSE105027, and GSE126677, respectively. The GSE151341 dataset, with a miRNA-sequencing platform, consisted of 41 early and 50 late knee OA plasma samples. The miRNA-sequencing platform yielded 2 OA synovial fluid samples and 3 healthy synovial fluid samples (GSE126677). The GSE105027 dataset, with an array sequencing platform, contained 12 OA chondrocyte serum samples and 12 healthy chondrocyte serum samples (Supplementary Table 1).

### Identifying differentially expressed microRNAs (DE-miRNAs)

The array databases were analyzed using the GEO2R (<https://www.ncbi.nlm.nih.gov/geo/geo2r>) database, and RNA/miRNA sequencing was analyzed using the limma and DESeq2 packages in the R software to identify DE-miRNAs. The main criterion for DE-miRNAs was log<sub>2</sub>foldchange (logFC) and adjusted P-value for each dataset. The results were visualized in volcano plots.

### Identifying overlapping DE-miRNAs in the OA biological fluid samples

A Venn diagram (<https://bioinfogp.cnb.csic.es/tools/venny/index.html>) was employed to identify overlapping DE-miRNAs in the OA biological fluid samples, encompassing knee OA plasma, chondrocyte serum, and synovial fluids. A specific miRNA was determined as an overlapping miRNA when it appeared at least in all 3 samples, and it was utilized for further analysis. All DE-miRNAs were pinpointed by comparing miRNA expression profiles between the OA and healthy controls.

### The gene ontology (GO) enrichment and Kyoto Encyclopedia of Genes and Genomes (KEGG) pathway analyses of overlapping DE-miRNAs and differentially expressed Genes

The GO and KEGG pathway analyses were performed using the mirPath v.3 (<https://dianalab.e-ce.uth.gr/html/mirpathv3/index.php?r=mirpath>) database on the overlapping DE-miRNAs.

### The network construction of common DE-miRNAs in all 3 datasets

The MIENTURENT database was drawn upon to construct the network of common DE-miRNAs in all 3 datasets and their target genes. The MIENTURENT database used the miRTarBase setting to construct the network. These analyses were performed with a false discovery rate of less than 0.05 and a minimum of 2 miRNA-target interactions.

The interaction of potential miRNAs' target genes was analyzed via STRING database ([https://stringdb.org/cgi/input?sessionId=bcF2bWZG131C&input\\_page\\_active\\_form=multiple\\_identifiers](https://stringdb.org/cgi/input?sessionId=bcF2bWZG131C&input_page_active_form=multiple_identifiers)).

### Statistical analysis

The significance of differences in the expression levels

of the selected genes and miRNAs was considered a P-value <0.05 as a statistical parameter. In addition, a P-value <0.05 was considered statistically significant in functional enrichment analysis.

## Results

### Identifying DE-miRNAs in the body fluids of human knee OA

Three datasets, namely GSE151341, GSE105027, and GSE126677, corresponding to late human knee OA plasma, chondrocyte serum, and synovial fluids, were analyzed using GEO2R to find DE-miRNAs.

The analysis of the GSE151341 dataset demonstrated 241 DE-miRNAs, of which 194 miRNAs showed upregulation and 47 downregulation (adjusted P<0.05 and logFC#1). The GSE105027 dataset analysis identified 52771 DE-miRNAs, with 21 miRNAs exhibiting upregulation and 52750 downregulation (adjusted P<0.05 and logFC#0.5). The GSE126677 dataset analysis revealed 369 DE-miRNAs, of which 38 miRNAs were upregulated and 331 downregulated (logFC#1). The distribution of DE-miRNAs in each dataset was visualized in corresponding Volcano plots (Figure 1A-C).

### Identifying overlapping DE-miRNAs in the body fluids of human knee OA

DE-miRNAs were sought in all 3 datasets. As is shown in the Venn diagram, 40 DE-miRNAs overlapped in the plasma, serum, and synovial fluids of OA patients (Figure 1D). Interestingly, the expression patterns of miRNAs in both plasma and serum were almost the same, whereas the patterns of these common miRNAs in the OA synovial fluid sample were reversed.

Among the 40 DE-miRNAs, in the late knee OA plasma

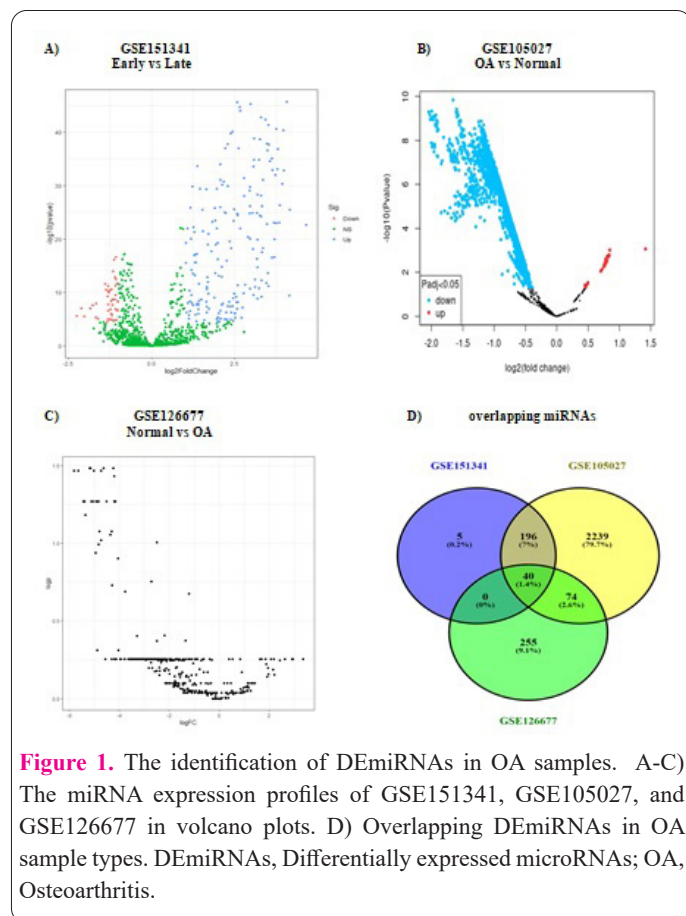


**Figure 1.** The identification of DE-miRNAs in OA samples. A-C) The miRNA expression profiles of GSE151341, GSE105027, and GSE126677 in volcano plots. D) Overlapping DE-miRNAs in OA sample types. DE-miRNAs, Differentially expressed microRNAs; OA, Osteoarthritis.

sample, while 36 miRNAs exhibited downregulation, 4 showed upregulation (hsa-miR-144-5p, hsa-miR-182-5p, hsa-miR-183-5p, and hsa-miR-192-5p). Further, in the OA chondrocyte serum sample, all 40 overlapping DE miRNAs showed downregulation. Additionally, in the OA synovial fluid sample, 38 miRNAs were upregulated, whereas 2 were downregulated (hsa-miR-146a-5p and hsa-miR-335-5p) (Table 1).

Further analysis was conducted on hsa-miR-146a-5p and hsa-miR-335-5p, differentially expressed and downregulated in all 3 OA plasma, serum, and synovial fluid

samples including finding their potential target genes and analyzing their related miRNA-target mRNA networks.

### The GO enrichment analysis of overlapping DE miRNAs

The GO enrichment analysis results are presented in supplementary Table 2A-C. The most enriched GO molecular functions were ion binding, nucleic acid-binding transcription factor activity, protein-binding transcription factor activity, enzyme binding, cytoskeletal protein binding, enzyme-regulator activity, RNA binding, and trans-

**Table 1.** List of overlapping DE miRNAs in OA. DE miRNAs, Differentially expressed microRNAs; OA, Osteoarthritis; Adj.P, Adjusted P-value; LogFC, Log2foldchange.

Overlapping DE miRNAs	GSE151341 (Late vs Early)	GSE105027 (OA vs Normal)	GSE126677 (OA vs Normal)
hsa-miR-1271-5p	Adj.P: 2.283849e-10 LogFC: -1.674047 (DOWN)	Adj.P: 0.0001931 LogFC: -0.68096 (DOWN)	Adj.P: 0.7950 LogFC: 2.0881 (UP)
hsa-miR-1301-3p	Adj.P: 1.762927e-18 LogFC: -1.708985 (DOWN)	Adj.P: 0.00010304 LogFC: -0.69834 (DOWN)	Adj.P: 0.63629 LogFC: 2.8234 (UP)
hsa-miR-1-3p	Adj.P: 3.746272e-08 LogFC: -1.657893 (DOWN)	Adj.P: 0.00003827 LogFC: -0.90335 (DOWN)	Adj.P: 0.79502 LogFC: 2.0085 (UP)
hsa-miR-146a-5p	Adj.P: 1.450013e-37 LogFC: -2.440440 (DOWN)	Adj.P: 0.00003827 LogFC: -0.84711 (DOWN)	Adj.P: 0.65302 LogFC: -2.1535745 (DOWN)
hsa-miR-148b-3p	Adj.P: 9.069115e-17 LogFC: -1.039974 (DOWN)	Adj.P: 0.00003827 LogFC: -0.86275 (DOWN)	Adj.P: 0.557744 LogFC: 2.461516 (UP)
hsa-miR-151a-5p	Adj.P: 4.274037e-13 LogFC: -1.295667 (DOWN)	Adj.P: 0.00003827 LogFC: -0.88037 (DOWN)	Adj.P: 0.42372 LogFC: 1.3414 (UP)
hsa-miR-181a-3p	Adj.P: 4.774050e-11 LogFC: -1.249582 (DOWN)	Adj.P: 0.00003827 LogFC: -0.85011 (DOWN)	Adj.P: 0.55774 LogFC: 3.40088 (UP)
hsa-miR-181d-5p	Adj.P: 1.789732e-19 LogFC: -1.958793 (DOWN)	Adj.P: 0.00003827 LogFC: -0.9132 (DOWN)	Adj.P: 0.557744 LogFC: 4.1125726 (UP)
hsa-miR-21-3p	Adj.P: 7.803143e-04 LogFC: -1.053403 (DOWN)	Adj.P: 0.00003827 LogFC: -0.87859 (DOWN)	Adj.P: 0.792930 LogFC: 2.13216 (UP)
hsa-miR-23b-3p	Adj.P: 3.922538e-31 LogFC: -1.378094 (DOWN)	Adj.P: 0.00003827 LogFC: -0.86004 (DOWN)	Adj.P: 0.5577447 LogFC: 3.21471 (UP)
hsa-miR-28-5p	Adj.P: 2.269351e-22 LogFC: -2.232284 (DOWN)	Adj.P: 0.00003827 LogFC: -0.83338 (DOWN)	Adj.P: 0.55774 LogFC: 2.657971 (UP)
hsa-miR-30e-3p	Adj.P: 2.733889e-27 LogFC: -1.223508 (DOWN)	Adj.P: 0.00001219 LogFC: -1.18785 (DOWN)	Adj.P: 0.09882 LogFC: 2.49339 (UP)
hsa-miR-3174	Adj.P: 3.195174e-05 LogFC: -2.102395 (DOWN)	Adj.P: 0.00003827 LogFC: -0.89804 (DOWN)	Adj.P: 0.557744 LogFC: 2.457297 (UP)
hsa-miR-329-5p	Adj.P: 2.580396e-08 LogFC: -3.225701 (DOWN)	Adj.P: 0.00003827 LogFC: -0.85166 (DOWN)	Adj.P: 0.55774 LogFC: 2.457297 (UP)
hsa-miR-335-3p	Adj.P: 1.463936e-41 LogFC: -2.652958 (DOWN)	Adj.P: 0.00004176 LogFC: -0.78704 (DOWN)	Adj.P: 0.55774 LogFC: 3.029492 (UP)
hsa-miR-335-5p	Adj.P: 3.300432e-28 LogFC: -2.162071 (DOWN)	Adj.P: 0.00003827 LogFC: -0.86507 (DOWN)	Adj.P: 0.55774 LogFC: -1.634774 (DOWN)
hsa-miR-337-3p	Adj.P: 1.337387e-15 LogFC: -3.043003 (DOWN)	Adj.P: 0.00003831 LogFC: -0.80859 (DOWN)	Adj.P: 0.55774 LogFC: 2.66954 (UP)
hsa-miR-340-5p	Adj.P: 7.835614e-27 LogFC: -1.640610 (DOWN)	Adj.P: 0.00003827 LogFC: -0.88619 (DOWN)	Adj.P: 0.17610 LogFC: 2.725214 (UP)
hsa-miR-342-5p	Adj.P: 5.131170e-07 LogFC: -1.194869 (DOWN)	Adj.P: 0.00000512 LogFC: -1.393 (DOWN)	Adj.P: 0.5674891 LogFC: 2.453260 (UP)
hsa-miR-3679-5p	Adj.P: 9.719165e-22 LogFC: -3.282502 (DOWN)	Adj.P: 0.00001164 LogFC: -1.04036 (DOWN)	Adj.P: 0.88951 LogFC: 1.415258 (UP)

hsa-miR-369-3p	Adj.P: 8.529282e-26 LogFC: - 3.172847 (DOWN)	Adj.P: 0.00003827 LogFC: -0.86793 (DOWN)	Adj.P: 0.0339987 LogFC: 5.641377 (UP)
hsa-miR-370-3p	Adj.P: 6.901492e-22 LogFC: - 3.246478 (DOWN)	Adj.P: 0.00003827 LogFC: -0.89828 (DOWN)	Adj.P: 0.557744 LogFC: 2.8810763 (UP)
hsa-miR-374b-3p	Adj.P: 5.785147e-06 LogFC: - 1.425690 (DOWN)	Adj.P: 0.00003827 LogFC: -0.83467 (DOWN)	Adj.P: 0.5577447 LogFC: 2.554790 (UP)
hsa-miR-376c-3p	Adj.P: 4.541860e-32 LogFC: - 3.544182 (DOWN)	Adj.P: 0.00003827 LogFC: -0.85212 (DOWN)	Adj.P: 0.5577447 LogFC: 3.231910 (UP)
hsa-miR-379-5p	Adj.P: 7.437957e-39 LogFC: - 3.512355 (DOWN)	Adj.P: 0.00003827 LogFC: -0.90999 (DOWN)	Adj.P: 0.5577447 LogFC: 3.942076 (UP)
hsa-miR-381-3p	Adj.P: 4.438984e-34 LogFC: - 3.478388 (DOWN)	Adj.P: 0.00003827 LogFC: -0.89021 (DOWN)	Adj.P: 0.795025 LogFC: 1.7518620 (UP)
hsa-miR-3928-3p	Adj.P: 1.418821e-03 LogFC: - 1.407792 (DOWN)	Adj.P: 0.00003827 LogFC: -0.85595 (DOWN)	Adj.P: 0.557744 LogFC: 2.928245 (UP)
hsa-miR-409-3p	Adj.P: 2.654750e-35 LogFC: - 3.464275 (DOWN)	Adj.P: 0.00003827 LogFC: -0.85653 (DOWN)	Adj.P: 0.663303 LogFC: 2.384578 (UP)
hsa-miR-409-5p	Adj.P: 6.797661e-18 LogFC: - 2.897052 (DOWN)	Adj.P: 0.00003625 LogFC: -0.92479 (DOWN)	Adj.P: 0.55774471 LogFC: 2.547922 (UP)
hsa-miR-411-5p	Adj.P: 2.021740e-30 LogFC: - 3.621818 (DOWN)	Adj.P: 0.00003827 LogFC: -0.86914 (DOWN)	Adj.P: 0.795025 LogFC: 1.9312881 (UP)
hsa-miR-425-3p	Adj.P: 1.671887e-23 LogFC: - 2.066326 (DOWN)	Adj.P: 0.00006428 LogFC: -0.74814 (DOWN)	Adj.P: 0.5577447 LogFC: 3.0257393 (UP)
hsa-miR-433-3p	Adj.P: 7.888549e-04 LogFC: - 2.242142 (DOWN)	Adj.P: 0.00003827 LogFC: -0.8457 (DOWN)	Adj.P: 0.55774471 LogFC: 2.7497783 (UP)
hsa-miR-493-3p	Adj.P: 8.499004e-28 LogFC: - 3.921990 (DOWN)	Adj.P: 0.00003827 LogFC: -0.88939 (DOWN)	Adj.P: 0.585855 LogFC: 2.72868057 (UP)
hsa-miR-656-3p	Adj.P: 1.027879e-06 LogFC: - 2.540577 (DOWN)	Adj.P: 0.00003827 LogFC: -0.86335 (DOWN)	Adj.P: 0.55774471 LogFC: 4.200735 (UP)
hsa-miR-671-3p	Adj.P: 9.647394e-43 LogFC: - 2.971678 (DOWN)	Adj.P: 0.00004193 LogFC: -0.77814 (DOWN)	Adj.P: 0.032845 LogFC: 5.14870034 (UP)
hsa-miR-889-3p	Adj.P: 1.413492e-30 LogFC: - 3.768896 (DOWN)	Adj.P: 0.00003827 LogFC: -0.85171 (DOWN)	Adj.P: 0.70501420 LogFC: 1.112212 (UP)
hsa-miR-144-5p	Adj.P: 2.396264e-04 LogFC: 1.235882	Adj.P: 0.00003827 LogFC: -0.8794 (DOWN)	Adj.P: 0.4883060 LogFC: 4.0393347 (UP)
hsa-miR-182-5p	Adj.P: 7.087762e-06 LogFC: 1.216693	Adj.P: 0.00003827 LogFC: -0.87345 (DOWN)	Adj.P: 0.5577447 LogFC: 3.084328 (UP)
hsa-miR-183-5p	Adj.P: 1.068509e-07 LogFC: 1.310801	Adj.P: 0.00003827 LogFC: -0.84196 (DOWN)	Adj.P: 0.8888540 LogFC: 1.1676541 (UP)
hsa-miR-192-5p	Adj.P: 8.977003e-06 LogFC: 1.000478	Adj.P: 0.00003827 LogFC: -0.84664 (DOWN)	Adj.P: 0.5755393 LogFC: 2.1143289 (UP)

membrane transporter activity. The most enriched GO biological processes were the cellular nitrogen compound metabolic process, the biosynthetic process, the cellular protein modification process, the small molecule metabolic process, the neurotrophin TRK receptor signaling pathway, the Fc- $\epsilon$  receptor signaling pathway, the blood coagulation process, the catabolic process, the epidermal growth factor receptor signaling pathway, the response to stress pathway, the cell death pathway, the Fc- $\gamma$  receptor signaling pathway involved in phagocytosis, the toll-like receptor signaling pathway, the immune system process, and the TRIF-dependent toll-like receptor signaling pathway. Additionally, the most enriched GO cellular components were the organelle, the protein complex, the cytosol, the nucleoplasm, the microtubule-organizing center, and the platelet  $\alpha$  granule lumen.

### The KEGG pathway analysis of overlapping DE miRNAs

The KEGG pathway analysis specified that the DE miRNAs were enriched in the following 12 signaling pathways: TGF- $\beta$ , adherens junction, Hippo, ErbB, Rap1, FoxO, PI3K-Akt, ubiquitin-mediated proteolysis, Ras, focal adhesion, actin cytoskeleton regulation, and mTOR (Table 2). The enriched miRNAs associated with the corresponding pathways are listed in Table 2.

### Construction of hsa-miR-146a-5p and hsa-miR-335-5p targeted genes network

Further analysis was done on hsa-miR-146a-5p and hsa-miR-335-5p, differentially expressed and downregulated in all 3 OA plasma, serum, and synovial fluid samples.

The target genes of hsa-miR-146a-5p and hsa-miR-

**Table 2.** KEGG pathway analysis on overlapping DE miRNAs. DE miRNAs, Differentially expressed microRNAs.

Pathway	P-value	Enriched miRNAs
TGF- $\beta$ signaling pathway (hsa04350)	1.81563938101e-06	hsa-miR-340-5p, hsa-miR-374b-3p, hsa-miR-656-3p, hsa-miR-335-3p, hsa-miR-369-3p, hsa-miR-379-5p, hsa-miR-381-3p, hsa-miR-23b-3p, hsa-miR-433-3p, hsa-miR-181d-5p, hsa-miR-337-3p, hsa-miR-376c-3p, hsa-miR-889-3p, hsa-miR-1271-5p, hsa-miR-370-3p, hsa-miR-1301-3p, hsa-miR-182-5p, hsa-miR-1-3p, hsa-miR-148b-3p, hsa-miR-3174, hsa-miR-493-3p, hsa-miR-409-3p, hsa-miR-183-5p, hsa-miR-146a-5p, hsa-miR-30e-3p, hsa-miR-21-3p, hsa-miR-3928-3p, hsa-miR-329-5p, hsa-miR-671-3p
Adherens junction (hsa04520)	4.1044602359e-06	hsa-miR-335-3p, hsa-miR-381-3p, hsa-miR-3928-3p, hsa-miR-183-5p, hsa-miR-148b-3p, hsa-miR-181d-5p, hsa-miR-30e-3p, hsa-miR-379-5p, hsa-miR-656-3p, hsa-miR-182-5p, hsa-miR-340-5p, hsa-miR-146a-5p, hsa-miR-23b-3p, hsa-miR-376c-3p, hsa-miR-369-3p, hsa-miR-1301-3p, hsa-miR-1-3p, hsa-miR-1271-5p, hsa-miR-409-3p, hsa-miR-28-5p, hsa-miR-889-3p, hsa-miR-433-3p, hsa-miR-493-3p, hsa-miR-21-3p, hsa-miR-337-3p
Hippo signaling pathway (hsa04390)	4.1044602359e-06	hsa-miR-335-3p, hsa-miR-369-3p, hsa-miR-656-3p, hsa-miR-182-5p, hsa-miR-1-3p, hsa-miR-381-3p, hsa-miR-409-5p, hsa-miR-183-5p, hsa-miR-379-5p, hsa-miR-146a-5p, hsa-miR-148b-3p, hsa-miR-28-5p, hsa-miR-370-3p, hsa-miR-192-5p, hsa-miR-23b-3p, hsa-miR-340-5p, hsa-miR-376c-3p, hsa-miR-889-3p, hsa-miR-337-3p, hsa-miR-409-3p, hsa-miR-1301-3p, hsa-miR-181d-5p, hsa-miR-30e-3p, hsa-miR-329-5p, hsa-miR-335-5p, hsa-miR-411-5p, hsa-miR-493-3p, hsa-miR-374b-3p, hsa-miR-3928-3p, hsa-miR-144-5p, hsa-miR-433-3p, hsa-miR-21-3p, hsa-miR-1271-5p, hsa-miR-3174, hsa-miR-3679-5p, hsa-miR-342-5p
ErbB signaling pathway (hsa04012)	7.07066574017e-06	hsa-miR-21-3p, hsa-miR-23b-3p, hsa-miR-3174, hsa-miR-374b-3p, hsa-miR-433-3p, hsa-miR-656-3p, hsa-miR-182-5p, hsa-miR-183-5p, hsa-miR-1301-3p, hsa-miR-335-3p, hsa-miR-381-3p, hsa-miR-181d-5p, hsa-miR-340-5p, hsa-miR-369-3p, hsa-miR-192-5p, hsa-miR-1271-5p, hsa-miR-379-5p, hsa-miR-493-3p, hsa-miR-1-3p, hsa-miR-148b-3p, hsa-miR-3679-5p, hsa-miR-30e-3p, hsa-miR-146a-5p, hsa-miR-889-3p, hsa-miR-337-3p, hsa-miR-409-3p, hsa-miR-3928-3p, hsa-miR-342-5p, hsa-miR-370-3p, hsa-miR-376c-3p, hsa-miR-671-3p, hsa-miR-329-5p, hsa-miR-144-5p, hsa-miR-28-5p, hsa-miR-409-5p
Rap1 signaling pathway (hsa04015)	1.05470815092e-05	hsa-miR-369-3p, hsa-miR-1271-5p, hsa-miR-340-5p, hsa-miR-1-3p, hsa-miR-148b-3p, hsa-miR-335-3p, hsa-miR-374b-3p, hsa-miR-409-3p, hsa-miR-493-3p, hsa-miR-656-3p, hsa-miR-181d-5p, hsa-miR-370-3p, hsa-miR-381-3p, hsa-miR-182-5p, hsa-miR-23b-3p, hsa-miR-335-5p, hsa-miR-342-5p, hsa-miR-30e-3p, hsa-miR-183-5p, hsa-miR-329-5p, hsa-miR-146a-5p, hsa-miR-337-3p, hsa-miR-433-3p, hsa-miR-3928-3p, hsa-miR-889-3p, hsa-miR-21-3p, hsa-miR-28-5p, hsa-miR-3174, hsa-miR-411-5p, hsa-miR-376c-3p, hsa-miR-3679-5p, hsa-miR-1301-3p, hsa-miR-144-5p, hsa-miR-379-5p, hsa-miR-192-5p
FoxO signaling pathway (hsa04068)	0.00043585883	hsa-miR-148b-3p, hsa-miR-335-3p, hsa-miR-340-5p, hsa-miR-369-3p, hsa-miR-381-3p, hsa-miR-889-3p, hsa-miR-183-5p, hsa-miR-3928-3p, hsa-miR-379-5p, hsa-miR-30e-3p, hsa-miR-656-3p, hsa-miR-23b-3p, hsa-miR-181d-5p, hsa-miR-370-3p, hsa-miR-493-3p, hsa-miR-337-3p, hsa-miR-409-3p, hsa-miR-1301-3p, hsa-miR-433-3p, hsa-miR-182-5p, hsa-miR-1271-5p, hsa-miR-21-3p, hsa-miR-146a-5p, hsa-miR-376c-3p, hsa-miR-1-3p, hsa-miR-3679-5p, hsa-miR-374b-3p, hsa-miR-3174, hsa-miR-329-5p, hsa-miR-342-5p, hsa-miR-411-5p, hsa-miR-28-5p, hsa-miR-144-5p
PI3K-Akt signaling pathway (hsa04151)	0.00043585883	hsa-miR-335-3p, hsa-miR-340-5p, hsa-miR-889-3p, hsa-miR-1-3p, hsa-miR-146a-5p, hsa-miR-376c-3p, hsa-miR-656-3p, hsa-miR-370-3p, hsa-miR-183-5p, hsa-miR-181d-5p, hsa-miR-21-3p, hsa-miR-23b-3p, hsa-miR-433-3p, hsa-miR-182-5p, hsa-miR-148b-3p, hsa-miR-337-3p, hsa-miR-369-3p, hsa-miR-381-3p, hsa-miR-379-5p, hsa-miR-1301-3p, hsa-miR-409-3p, hsa-miR-28-5p, hsa-miR-3679-5p, hsa-miR-493-3p, hsa-miR-1271-5p, hsa-miR-342-5p, hsa-miR-30e-3p, hsa-miR-3928-3p, hsa-miR-3174, hsa-miR-409-5p, hsa-miR-335-5p, hsa-miR-329-5p, hsa-miR-374b-3p, hsa-miR-144-5p, hsa-miR-192-5p, hsa-miR-425-3p, hsa-miR-671-3p
Ubiquitin-mediated proteolysis (hsa04120)	0.00110723662	hsa-miR-335-3p, hsa-miR-340-5p, hsa-miR-381-3p, hsa-miR-433-3p, hsa-miR-656-3p, hsa-miR-889-3p, hsa-miR-181d-5p, hsa-miR-23b-3p, hsa-miR-369-3p, hsa-miR-1-3p, hsa-miR-376c-3p, hsa-miR-493-3p, hsa-miR-146a-5p, hsa-miR-148b-3p, hsa-miR-3679-5p, hsa-miR-182-5p, hsa-miR-409-3p, hsa-miR-192-5p, hsa-miR-409-5p, hsa-miR-183-5p, hsa-miR-21-3p, hsa-miR-379-5p, hsa-miR-411-5p, hsa-miR-370-3p, hsa-miR-1301-3p, hsa-miR-374b-3p, hsa-miR-3174, hsa-miR-28-5p, hsa-miR-3928-3p, hsa-miR-1271-5p, hsa-miR-30e-3p, hsa-miR-335-5p, hsa-miR-337-3p
Ras signaling pathway (hsa04014)	0.00138078699	hsa-miR-23b-3p, hsa-miR-28-5p, hsa-miR-335-3p, hsa-miR-3679-5p, hsa-miR-493-3p, hsa-miR-656-3p, hsa-miR-381-3p, hsa-miR-411-5p, hsa-miR-182-5p, hsa-miR-340-5p, hsa-miR-369-3p, hsa-miR-1301-3p, hsa-miR-148b-3p, hsa-miR-30e-3p, hsa-miR-329-5p, hsa-miR-889-3p, hsa-miR-1271-5p, hsa-miR-409-5p, hsa-miR-183-5p, hsa-miR-370-3p, hsa-miR-337-3p, hsa-miR-409-3p, hsa-miR-1-3p, hsa-miR-181d-5p, hsa-miR-335-5p, hsa-miR-374b-3p, hsa-miR-433-3p, hsa-miR-671-3p, hsa-miR-342-5p, hsa-miR-146a-5p, hsa-miR-21-3p, hsa-miR-3928-3p, hsa-miR-144-5p, hsa-miR-3174, hsa-miR-379-5p, hsa-miR-376c-3p

Focal adhesion (hsa04510)	0.00138078699	hsa-miR-148b-3p, hsa-miR-23b-3p, hsa-miR-335-3p, hsa-miR-340-5p, hsa-miR-656-3p, hsa-miR-889-3p, hsa-miR-183-5p, hsa-miR-369-3p, hsa-miR-381-3p, hsa-miR-192-5p, hsa-miR-493-3p, hsa-miR-409-3p, hsa-miR-3679-5p, hsa-miR-376c-3p, hsa-miR-182-5p, hsa-miR-671-3p, hsa-miR-30e-3p, hsa-miR-342-5p, hsa-miR-3174, hsa-miR-146a-5p, hsa-miR-181d-5p, hsa-miR-337-3p, hsa-miR-1271-5p, hsa-miR-3928-3p, hsa-miR-329-5p, hsa-miR-370-3p, hsa-miR-433-3p, hsa-miR-374b-3p, hsa-miR-1301-3p, hsa-miR-1-3p, hsa-miR-379-5p, hsa-miR-335-5p, hsa-miR-425-3p, hsa-miR-28-5p, hsa-miR-21-3p, hsa-miR-409-5p
Regulation of actin cytoskeleton (hsa04810)	0.0016593089	hsa-miR-146a-5p, hsa-miR-28-5p, hsa-miR-433-3p, hsa-miR-335-3p, hsa-miR-3679-5p, hsa-miR-381-3p, hsa-miR-493-3p, hsa-miR-148b-3p, hsa-miR-181d-5p, hsa-miR-23b-3p, hsa-miR-656-3p, hsa-miR-1271-5p, hsa-miR-337-3p, hsa-miR-340-5p, hsa-miR-369-3p, hsa-miR-183-5p, hsa-miR-182-5p, hsa-miR-1301-3p, hsa-miR-889-3p, hsa-miR-30e-3p, hsa-miR-342-5p, hsa-miR-1-3p, hsa-miR-409-5p, hsa-miR-3174, hsa-miR-379-5p, hsa-miR-3928-3p, hsa-miR-376c-3p, hsa-miR-370-3p, hsa-miR-409-3p, hsa-miR-192-5p, hsa-miR-144-5p, hsa-miR-425-3p, hsa-miR-21-3p, hsa-miR-329-5p
mTOR signaling pathway (hsa04150)	0.002388425	hsa-miR-335-3p, hsa-miR-337-3p, hsa-miR-340-5p, hsa-miR-369-3p, hsa-miR-381-3p, hsa-miR-409-3p, hsa-miR-433-3p, hsa-miR-656-3p, hsa-miR-183-5p, hsa-miR-28-5p, hsa-miR-3174, hsa-miR-342-5p, hsa-miR-374b-3p, hsa-miR-182-5p, hsa-miR-376c-3p, hsa-miR-889-3p, hsa-miR-148b-3p, hsa-miR-181d-5p, hsa-miR-23b-3p, hsa-miR-3928-3p, hsa-miR-144-5p, hsa-miR-1-3p, hsa-miR-493-3p, hsa-miR-1271-5p, hsa-miR-30e-3p, hsa-miR-329-5p, hsa-miR-21-3p, hsa-miR-3679-5p, hsa-miR-1301-3p, hsa-miR-146a-5p, hsa-miR-671-3p, hsa-miR-370-3p

335-5p, which were downregulated in all 3 OA fluid samples were sought; then, a network was constructed in the MIENTURNET database, which employed the miR-TarBase setting.

The results demonstrated that hsa-miR-146a-5p could target the *PLAUR*, *NFAT5*, *CCND2*, *LFNG*, *IL6*, *PTGS2*, *ICAM1*, *NUMB*, *LICAM*, *SLP1*, *TLR4*, *MTA2*, *EGFR*, *CDKN1A*, *CXCL8*, *BRCA1*, *ROCK1*, *TLR2*, *IRAK2*, and *CXCR4* genes (Figure 2), while hsa-miR-335-5p could target the *PLAUR*, *BRCA1*, *ROCK*, and *CXCR4* genes (Figure 2).

In addition, hsa-miR-146a-5p and hsa-miR-335-5p might play roles in almost all the mentioned signaling pathways, namely TGF- $\beta$ , adherens junction, Hippo, ErbB, Rap1, FoxO, PI3K-Akt, ubiquitin-mediated proteolysis, Ras, focal adhesion, actin cytoskeleton regulation, and mTOR (highlighted in Table 2).

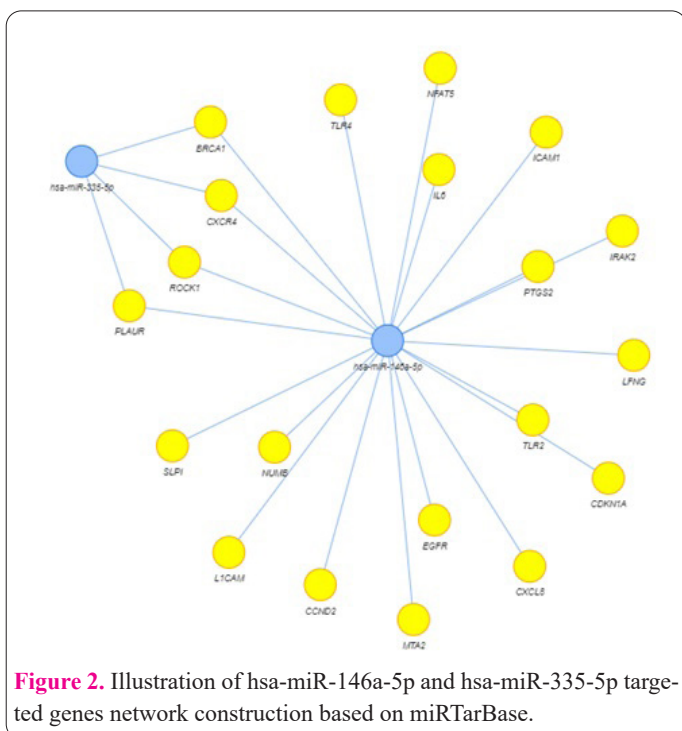


Figure 2. Illustration of hsa-miR-146a-5p and hsa-miR-335-5p targeted genes network construction based on miRTarBase.

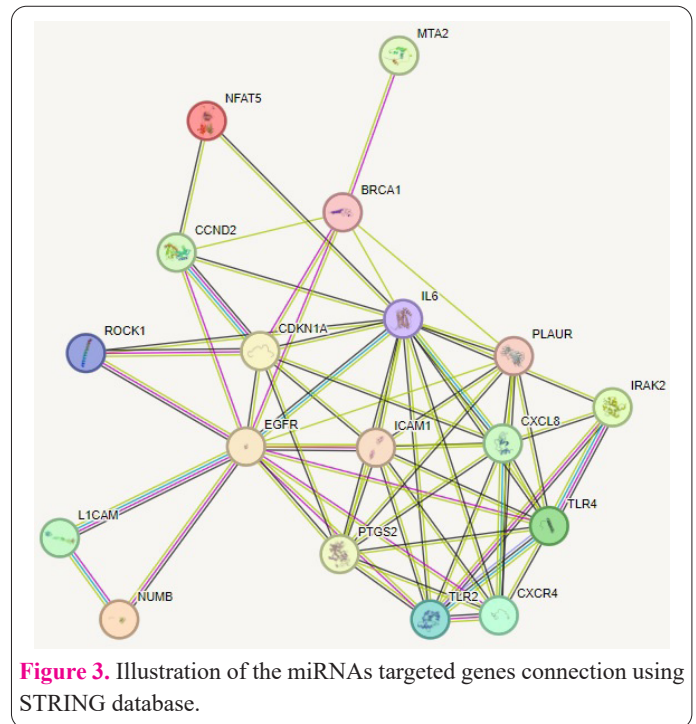


Figure 3. Illustration of the miRNAs targeted genes connection using STRING database.

In addition, we analyzed the interaction of hsa-miR-146a-5p and hsa-miR-335-5p target genes via the STRING database. The outcomes exhibited the connection of the target genes in different pathways and some of them including *IL6*, *PLAUR*, *PTGS2* and *EGFR* were important hub gene among target genes connection which probably suggest that they might have significant roles in OA pathogenesis (Figure 3).

### Discussion

OA, a common musculoskeletal disorder, is a multifactorial degenerative disease with considerable socio-economic impacts. It happens when the cartilage or the cushion between the joints breaks down, causing pain, swelling, and stiffness (7). Research has highlighted miRNAs as novel regulators in OA with great potential as diagnos-

tic biomarkers (13, 14). Analysis of human body fluids is fundamentally challenging owing to their unique characteristics. Nevertheless, remarkable advances in sample preparation methods and new quantification technologies have made body fluid analysis less invasive and more advantageous in providing fresh insights into OA (11, 12).

In the present study, we investigated miRNAs and their relative pathways in the body fluids of human knee OA based on bioinformatics analysis. Generally, gene expression profiles derived from OA plasma, chondrocyte serum, and synovial fluid samples are analyzed to determine overlapping DE miRNAs according to the GEO database. The current investigation seems to be the first to identify overlapping DE miRNAs in the body fluids of human knee OA (plasma, serum, and synovial fluids).

Having identified DE miRNAs in the different fluids, we determined the overlapping miRNAs with a Venn diagram. We identified 40 DE miRNAs in all 3 datasets as the most overlapping miRNAs. The expression patterns of the DE miRNAs in both plasma and serum were almost similar, whereas the patterns of these common DE miRNAs in the OA synovial fluid sample were reversed. The difference in nature of the samples (synovial fluid, serum and plasma), may be one of the reasons for such differences in the gene expression pattern. We considered 2 DE miRNAs, hsa-miR-146a-5p and hsa-miR-335-5p, which exhibited a similar expression pattern (downregulation) in all 3 plasma, serum, and synovial fluid samples, as potential OA biomarkers.

In the pathogenesis of OA, extensive research has revealed that miR-146a promotes chondrocyte apoptosis, cartilage damage, inflammation, and neovascularization (14, 15).

Several studies have compared the expression pattern between OA and healthy tissues and demonstrated the role of miRNA-altered expression patterns in OA (16). Still, reports are conflicting vis-à-vis the expression patterns of miR-146 in OA patients' tissues and body fluids.

Kusnierova et al (17) found that miR-146a-5p, miR-223-3p, and miR-23a-3p could constitute a significant group of biomarkers for the detection of various pathophysiological conditions, such as inflammatory conditions, in synovial fluids.

A study reported that the circulating miR-146a level was upregulated in OA patients, while the expression level of miR-145a in OA patients' cartilage and bone tissues was meaningfully downregulated (18). Another investigation reported that miR-146a was overexpressed in mild OA cartilage (grade I) and underexpressed in moderate-to-severe OA (18). In the exosome of the synovial fluid, miR-146a expression was high in the early stages of OA and low in the later stages, according to another study (19). In some other investigations, miR-146a expression was considerably higher in the cartilage tissue of OA patients than that in non-OA controls; nonetheless, miR-146a expression in the synoviocytes of OA patients was significantly low compared with non-OA individuals (16, 20). Our analysis revealed that miR-146a-5p expression was significantly downregulated in all 3 OA synovial, plasma, and serum fluid samples. Rousseau et al (21) demonstrated that miR-146a-5p expression was high in the serum of female OA patients in comparison with male counterparts. Wu et al (22) reported the overexpression of miR-146a-5p and miR-365 in OA patients' plasma.

Our results are discordant with the previous reports of upregulation in miR-146a-5p in OA patients' serum and plasma. Previous investigations suggesting upregulated miR-146a expression as a circulating biomarker of OA (21, 23) are limited by their sample size of control individuals and their screening of only women, hence the need for further research on the diagnostic accuracy of plasma and serum concerning OA.

Some target genes of miR-146a, namely Bcl-2, TRAF6, IRAK1, VEGF, Smad4, and TGF- $\beta$ , have been linked to OA pathophysiology (23-28). However, our results predicted some more genes, namely PLAUR, NFAT5, CCND2, LFNG, IL6, PTGS2, ICAM1, NUMB, L1CAM, SLP1, TLR4, MTA2, EGFR, CDKN1A, CXCL8, BRCA1, ROCK1, TLR2, IRAK2, and CXCR4, as targets of miR-146a-5p. These findings should be experimentally confirmed, especially with respect to their interactions and mechanisms apropos of OA pathophysiology. Notably, some predicted targets, including IL-6, PTGS2, NUMB, TLR4, EGFR, and TLR-2, have been documented to exhibit dysregulation in OA and play roles in OA pathophysiology (29-34).

Wang et al (29) found that the SDF-1/CXCR4 signaling pathway in vivo reduced the mRNA expression of MMP-3, MMP-9, and MMP-13, slowed the degradation of type II collagen and aggrecan in cartilage tissue, and lessened the degeneration of cartilage tissue in an OA disease model. Some studies have concluded that IL-6 is associated with an increased risk of OA development (30, 35, 36). Jin et al (31) reported that miR-26a-5p was downregulated and PTGS2 was upregulated in the synovial fibroblasts of OA. The downregulation of miR-146a-5p could suppress the apoptosis and promote the autophagy of chondrocytes by targeting NUMB in vivo and in vitro (32). Raimo et al (37) demonstrated that miR-146a directed the targeting of LFNG and NUMB, leading to NOTCH1 signaling activation.

Blocking TLR4 in the joints could effectively attenuate OA progression and diminish pain (33). Zhang et al (34) demonstrated a primarily protective role for EGFR during OA progression through chondrocyte survival regulation and cartilage degradation. The TLR-2/NF- $\kappa$ B signaling pathway could contribute to degenerative knee OA (38). Duan et al (39) found that miR-146a-5p-riched exosomes released from bone-marrow-derived mesenchymal stem cells could offer neuroprotection by reducing neuronal apoptosis and inflammation associated with NFAT5 suppression. Li et al (40) revealed that inhibiting the expression of CCND1 and CCND2 could suppress the proliferation and cell cycle progression in non-small cell lung cancer cells.

Cyclooxygenase-2 (COX2), encoded by the PTGS2 gene, is a significant inflammatory mediator in several diseases and a target for miR-146a-5p in bone marrow-derived mesenchymal stem cells (41). Moreover, miR-146a-5p could target ICAM1, IL6, NFKB1, PLAUR, PTGS2, RHOA, ROCK1, SPP1, TGFB1, TLR2, and TLR4, associated with atherosclerosis development (42).

Chen et al (43) concluded that miR-146a in non-small-cell lung carcinoma cells inhibited cell proliferation and metastasis and induced apoptosis via the EGFR signaling pathway. Furthermore, miR-146a-5p could promote prostate cancer cell apoptosis by targeting ROCK1 (44). Wotschovsky et al (45) showed that CXCL8/IL8, UHRF1,

MCM10, and CDKN3 were downregulated and targeted by miR-146a-5p. Garcia et al (46) revealed the downregulation of BRCA1 expression by miR-146a and miR-146b-5p in triple-negative sporadic breast cancers. In Alzheimer's disease, miR-146a could suppress ROCK1 expression (47). Our results concerning the targets of miR-146a-5p and their regulatory roles in OA require clarification in terms of the exact mechanisms of miR-146a and the direct targets involved in the different stages of OA. Nevertheless, our results confirm the role of miR-146a-5p in OA and nominate miR-146a-5p expression as a candidate OA biomarker.

Some studies have unraveled the role of miR-335-5p in OA pathogenesis. The expression of miR-335-5p exhibits upregulation in OA patients' cartilage (20). Tornero-Esteban et al (48) stated that miR-335-5p had a role during osteogenic differentiation and reported a correlation between miR-335-5p expression alterations and OA features. According to Lu et al (49), miR-335-5p could target the HBP1 gene, mediate chondrocyte apoptosis, and promote chondrocyte apoptosis, thereby playing a role in OA development. Zhong et al (50) indicated that miR-335-5p expression was meaningfully downregulated in OA chondrocytes compared with healthy chondrocytes. They also reported that miR-335-5p overexpression could elevate viability and autophagy-related factors and diminish inflammatory mediators in human OA chondrocytes, denoting that miRNA-335-5p could markedly ameliorate inflammation in human OA chondrocytes by triggering autophagy. Our results deciphered miR-335p downregulation in all 3 examined fluids of human OA patients (serum, plasma, and synovial fluids). Our literature search yielded no report of miR-335-5p expression in OA patients' serum, plasma, and synovial fluids. However, miR-335-5p downregulation is in line with a previous report of its expression in chondrocytes and in contrast with its expression in OA patients' cartilage.

Our target analysis of miR-335-5p indicated PLAUR, BRCA1, ROCK1, and CXCR4 as candidate miR-335-5p targets. Both PLAUR and CDH11 could predict the overexpression of miR-335 targets in gastric cancer tissues (51). Wang et al (52) found that miR-335 acted as a tumor suppressor by targeting ROCK1 and inhibiting osteosarcoma cell migration and invasion. To our knowledge, however, none of the previous investigations has demonstrated interactions between miR-335-5p and PLAUR, BRCA1, and CXCR4, except for ROCK1. More experimental research is warranted concerning these targets and their role in OA pathogenesis.

The overlapping DE miRNAs in our KEGG pathway analysis exhibited enrichment in the following signaling pathways: TGF- $\beta$ , adherens junction, Hippo, ErbB, Rap1, FoxO, PI3K-Akt, ubiquitin-mediated proteolysis, Ras, focal adhesion, actin cytoskeleton regulation, and mTOR. Both hsa-miR-146a-5p and hsa-miR-335-5p played a role in all the mentioned pathways.

The TGF- $\beta$  signaling pathway stimulates chondrocyte proliferation while inhibiting chondrocyte hypertrophy and maturation. Several studies have suggested that the TGF- $\beta$ /Smad pathway plays a critical role in regulating articular chondrocyte hypertrophy and maturation during OA development (53-55). Substantial evidence indicates that the Hippo signaling pathway can interact with the

TGF- $\beta$  and NF- $\kappa$ B signaling pathways, participate in OA development, and control cartilage morphology by regulating the extracellular matrix (56-58). The FoxO signaling pathway is closely involved in chondrocyte dysfunction and OA pathogenesis owing to the protective role of FoxO in oxidative stress. FoxO could also regulate chondrocyte autophagy, chondrocyte maturation, and aging, all of which contribute to OA development (59-63). The PI3K/Akt signaling pathway is associated with TNF- $\alpha$ , which may be involved in OA pathogenesis. Moreover, PI3K/Akt activation could induce a series of downstream signaling pathways and target proteins, including NF- $\kappa$ B and MMPs, which are significant catabolic markers in OA (64, 65). The mTOR signaling pathway is essential for joint health and is correlated with OA pathogenesis. The upregulation of mTOR in OA cartilage is linked to increased chondrocyte apoptosis (66, 67).

Alongside the mentioned validated OA signaling pathways, studies on the signaling pathways of adherens junction, ErbB, Rap1, ubiquitin-mediated proteolysis, Ras, focal adhesion, which our team recently reported (68), and actin cytoskeleton regulation in OA pathogenesis are limited, and the roles of these pathways need experimental clarification.

### Limitations

The outcomes of the present study should be defined in light of its limitations. First, the analyzed three datasets in the present study were the only available published data sets for the body fluids of OA at the time of our investigation. Most of the datasets were related to the tissues of OA.

In addition, experimental analysis should be done to validate bioinformatics analysis in this study in serum, plasma and synovial fluids of OA patients' samples.

### Conclusions

The present study provides a comprehensive bioinformatics analysis of key miRNAs and signaling pathways among OA patients and is the first investigation to compare DE miRNAs between human knee OA serum, plasma, and synovial fluid samples. Our data suggested that the dysregulation of hsa-miR-335-5p and hsa-miR-146a-5p could serve as a noninvasive clinical utility OA biomarker. Therefore, miRNA-335-5p and hsa-miR-146a-5p have the potential for future application in the clinical diagnosis and treatment of OA.

The downregulation of hsa-miR-146a-5p and hsa-miR-335-5p was identified in all 3 types of biological fluid samples of OA. Thus, we recommend the experimental validation of these 2 miRNAs throughout OA stages in the biological fluid and tissue samples and peripheral blood mononuclear cells of OA patients compared with healthy controls. Since our work is limited to the analysis of only a dataset of OA serum, plasma, and synovial fluids, it is advisable that the expression patterns of these 2 miRNAs and all other overlapping miRNAs be analyzed in more datasets of body fluids to confirm our results.

Human samples, including human body fluids, are of great interest to researchers given the potential significance of translational medicine. Accordingly, we hope that our findings offer fresh insights into the human body fluid analysis of OA concerning miRNA expression.

## References

1. Goldring MB, Otero M. Inflammation in osteoarthritis. *Curr Opin Rheumatol* 2011;23(5):471.
2. Sinusas K. Osteoarthritis: diagnosis and treatment. *AFP* 2012;85(1):49-56.
3. Monemdjou R, Kapoor M. Synovium in the pathophysiology of osteoarthritis. *Clin Pract* 2010;7(6):661.
4. Zhang W, Qi L, Chen R, He J, Liu Z, Wang W, et al. Circular RNAs in osteoarthritis: indispensable regulators and novel strategies in clinical implications. *Arthritis Res Ther* 2021;23(1):1-15.
5. Hunter DJ, Schofield D, Callander E. The individual and socioeconomic impact of osteoarthritis. *Nat Rev Rheumatol* 2014;10(7):437-41.
6. Skou ST, Roos EM. Physical therapy for patients with knee and hip osteoarthritis: supervised, active treatment is current best practice. *Clin Exp Rheumatol*. 2019;37(suppl 120):112-17.
7. Glyn-Jones S, Palmer A, Agricola, R.; Price, AJ; Vincent, TL; Weinans, H.; Carr. *AJ Osteoarthritis Lancet*. 2015;386(9991):376-87.
8. Bennell K, Hall M, Hinman R. Osteoarthritis year in review 2015: rehabilitation and outcomes. *Osteoarthr Cartil* 2016;24(1):58-70.
9. Kang Y-J, Yoo J-I, Baek K-W. Differential gene expression profile by RNA sequencing study of elderly osteoporotic hip fracture patients with sarcopenia. *J Orthop Transl* 2021;29:10-8.
10. Karlsson C, Dehne T, Lindahl A, Brittberg M, Pruss A, Sittlinger M, et al. Genome-wide expression profiling reveals new candidate genes associated with osteoarthritis. *Osteoarthr Cartil* 2010;18(4):581-92.
11. Su S-B, Poon TCW, Thongboonkerd V. *Human body fluid*. Hindawi 2013.
12. Hu S, Loo JA, Wong DT. Human body fluid proteome analysis. *Proteomics* 2006;6(23):6326-53.
13. Oliviero A, Della Porta G, Peretti GM, Maffulli N. MicroRNA in osteoarthritis: physiopathology, diagnosis and therapeutic challenge. *Br Med Bull* 2019;130(1):137-47.
14. Malemud CJ. MicroRNAs and osteoarthritis. *Cells* 2018;7(8):92.
15. Hesari R, Keshvarinia M, Kabiri M, Rad I, Parivar K, Hoseinpoor H, et al. Comparative impact of platelet rich plasma and transforming growth factor- $\beta$  on chondrogenic differentiation of human adipose derived stem cells. *BioImpacts: BI* 2020;10(1):37.
16. Liu J-N, Lu S, Fu C-M. MiR-146a expression profiles in osteoarthritis in different tissue sources: a meta-analysis of observational studies. *J Orthop Surg Res* 2022;17(1):1-10.
17. Kušnierová P, Bystroňová I, Walder P, Hlubek R, Stejskal D. Contribution of miRNAs and Other Inflammatory Biomarkers to the Differentiation of Inflammatory and Non-Inflammatory Joint Effusions. *Acta Chir Orthop Traumatol* 2021;88(5):344-53.
18. Yamasaki K, Nakasa T, Miyaki S, Ishikawa M, Deie M, Adachi N, et al. Expression of MicroRNA-146a in osteoarthritis cartilage. *ACR* 2009;60(4):1035-41.
19. Liu D-H, Jheng Y-C, Chen P-Y, Yarmishyn AA, Huang S-E, Chien C-S, et al. Frontier review of the roles of exosomes in osteoarthritis. *J Chin Med Assoc* 2021;84(8):754-6.
20. Kopańska M, Szala D, Czech J, Gabło N, Gargasz K, Trzeciak M, et al. MiRNA expression in the cartilage of patients with osteoarthritis. *J Orthop Surg Res* 2017;12(1):1-7.
21. Rousseau J-C, Millet M, Croset M, Sornay-Rendu E, Borel O, Chapurlat R. Association of circulating microRNAs with prevalent and incident knee osteoarthritis in women: the OFELY study. *Arthritis Res Ther* 2020;22(1):1-12.
22. Wu W, Xuan Y, Ge Y, Mu S, Hu C, Fan R. Plasma miR-146a and miR-365 expression and inflammatory factors in patients with osteoarthritis. *Malays J Pathol*. 2021;43(2):311-7.
23. Skrzypa M, Szala D, Gabło N, Czech J, Pajak J, Kopanska M, et al. miRNA-146a-5p is upregulated in serum and cartilage samples of patients with osteoarthritis. *Pol. J Surg* 2019;91:1-5.
24. Soyocak A, Kurt H, Ozgen M, Cosan DT, Colak E, Gunes HV. miRNA-146a, miRNA-155 and JNK expression levels in peripheral blood mononuclear cells according to grade of knee osteoarthritis. *Gene* 2017;627:207-11.
25. Okuhara A, Nakasa T, Shibuya H, Niimoto T, Adachi N, Deie M, et al. Changes in microRNA expression in peripheral mononuclear cells according to the progression of osteoarthritis. *Mod Rheumatol* 2012;22(3):446-57.
26. Zhang F, Wang J, Chu J, Yang C, Xiao H, Zhao C, et al. MicroRNA-146a induced by hypoxia promotes chondrocyte autophagy through Bcl-2. *Cell Physiol Biochem* 2015;37(4):1442-53.
27. Jin L, Zhao J, Jing W, Yan S, Wang X, Xiao C, et al. Role of miR-146a in human chondrocyte apoptosis in response to mechanical pressure injury in vitro. *Int J Mol Med* 2014;34(2):451-63.
28. Houard X, Goldring MB, Berenbaum F. Homeostatic mechanisms in articular cartilage and role of inflammation in osteoarthritis. *Curr Rheumatol Rep* 2013;15(11):1-10.
29. Wang K, Li Y, Han R, Cai G, He C, Wang G, et al. T140 blocks the SDF-1/CXCR4 signaling pathway and prevents cartilage degeneration in an osteoarthritis disease model. *PloS one* 2017;12(4):e0176048.
30. Yang H, Zhou X, Xu D, Chen G. The IL-6 rs12700386 polymorphism is associated with an increased risk of developing osteoarthritis in the knee in the Chinese Han population: a case-control study. *BMC Med Genet* 2020;21(1):1-7.
31. Jin Z, Ren J, Qi S. Human bone mesenchymal stem cells-derived exosomes overexpressing microRNA-26a-5p alleviate osteoarthritis via down-regulation of PTGS2. *Int Immunopharmacol* 2020;78:105946.
32. Zhang H, Zheng W, Li D, Zheng J. miR-146a-5p promotes chondrocyte apoptosis and inhibits autophagy of osteoarthritis by targeting NUMB. *Cartil* 2021;13(2\_suppl):1467S-77S.
33. Park S, Shin H-J, Shah M, Cho H-Y, Anwar MA, Achek A, et al. TLR4/MD2 specific peptides stalled in vivo LPS-induced immune exacerbation. *Biomater* 2017;126:49-60.
34. Zhang X, Zhu J, Liu F, Li Y, Chandra A, Levin LS, et al. Reduced EGFR signaling enhances cartilage destruction in a mouse osteoarthritis model. *Bone Res* 2014;2(1):1-12.
35. Wiegertjes R, van de Loo FA, Blaney Davidson EN. A roadmap to target interleukin-6 in osteoarthritis. *Rheumatology* 2020;59(10):2681-94.
36. Liao Y, Ren Y, Luo X, Mirando AJ, Long JT, Leinroth A, et al. Interleukin-6 signaling mediates cartilage degradation and pain in posttraumatic osteoarthritis in a sex-specific manner. *Sci Signal* 2022;15(744):eabn7082.
37. Raimo M, Orso F, Grassi E, Cimino D, Penna E, De Pittà C, et al. miR-146a exerts differential effects on melanoma growth and metastatization. *Mol Cancer Res* 2016;14(6):548-62.
38. Liu Y-X, Wang G-D, Wang X, Zhang Y-L, Zhang T-L. Effects of TLR-2/NF- $\kappa$ B signaling pathway on the occurrence of degenerative knee osteoarthritis: an in vivo and in vitro study. *Oncotarget* 2017;8(24):38602.
39. Duan S, Wang F, Cao J, Wang C. Exosomes derived from MicroRNA-146a-5p-enriched bone marrow mesenchymal stem cells alleviate intracerebral hemorrhage by inhibiting neuronal apoptosis and microglial M1 polarization. *Drug Des Devel Ther* 2020;14:3143.
40. Li Y-L, Wang J, Zhang C-Y, Shen Y-Q, Wang H-M, Ding L, et al. MiR-146a-5p inhibits cell proliferation and cell cycle progression in NSCLC cell lines by targeting CCND1 and CCND2. *Oncotarget* 2016;7(37):59287.

41. Matysiak M, Fortak-Michalska M, Szymanska B, Orłowski W, Jurewicz A, Selmaj K. MicroRNA-146a negatively regulates the immunoregulatory activity of bone marrow stem cells by targeting prostaglandin E2 synthase-2. *J Immunol* 2013;190(10):5102-9.
42. Chatzopoulou F, Kyritsis KA, Papagiannopoulos CI, Galatou E, Mittas N, Theodoroula NF, et al. Dissecting miRNA–Gene Networks to Map Clinical Utility Roads of Pharmacogenomics-Guided Therapeutic Decisions in Cardiovascular Precision Medicine. *Cells* 2022;11(4):607.
43. Chen G, Umelo IA, Lv S, Teugels E, Fostier K, Kronenberger P, et al. miR-146a inhibits cell growth, cell migration and induces apoptosis in non-small cell lung cancer cells. *PLoS one* 2013;8(3):e60317.
44. Xu B, Huang Y, Niu X, Tao T, Jiang L, Tong N, et al. Hsa-miR-146a-5p modulates androgen-independent prostate cancer cells apoptosis by targeting ROCK1. *The Prostate* 2015;75(16):1896-903.
45. Wotschovsky Z, Gummlich L, Liep J, Stephan C, Kilic E, Jung K, et al. Integrated microRNA and mRNA signature associated with the transition from the locally confined to the metastasized clear cell renal cell carcinoma exemplified by miR-146-5p. *PLoS one* 2016;11(2):e0148746.
46. Garcia AI, Buisson M, Bertrand P, Rimokh R, Rouleau E, Lopez BS, et al. Down-regulation of BRCA1 expression by miR-146a and miR-146b-5p in triple negative sporadic breast cancers. *EMBO Mol Med* 2011;3(5):279-90.
47. Wang G, Huang Y, Wang L-L, Zhang Y-F, Xu J, Zhou Y, et al. MicroRNA-146a suppresses ROCK1 allowing hyperphosphorylation of tau in Alzheimer’s disease. *Sci Rep* 2016;6(1):1-12.
48. Tornero-Esteban P, Rodríguez-Rodríguez L, Abásolo L, Tomé M, López-Romero P, Herranz E, et al. Signature of microRNA expression during osteogenic differentiation of bone marrow MSCs reveals a putative role of miR-335-5p in osteoarthritis. *BMC Musculoskelet. Disord* 2015;16(1):1-9.
49. Lu X, Li Y, Chen H, Pan Y, Lin R, Chen S. miR-335-5P contributes to human osteoarthritis by targeting HBP1. *Exp Ther Med* 2021;21(2):1-.
50. Zhong G, Long H, Ma S, Shunhan Y, Li J, Yao J. miRNA-335-5p relieves chondrocyte inflammation by activating autophagy in osteoarthritis. *Life Sci* 2019;226:164-72.
51. Sandoval-Bórquez A, Polakovicova I, Carrasco-Véliz N, Lobos-González L, Riquelme I, Carrasco-Avino G, et al. MicroRNA-335-5p is a potential suppressor of metastasis and invasion in gastric cancer. *Clin. Epigenetics* 2017;9(1):1-16.
52. Wang Y, Zhao W, Fu Q. miR-335 suppresses migration and invasion by targeting ROCK1 in osteosarcoma cells. *Mol Cell Biochem* 2013;384(1):105-11.
53. van der Kraan PM, van den Berg WB. Osteophytes: relevance and biology. *Osteoarthr. Cartil* 2007;15(3):237-44.
54. Shen J, Li J, Wang B, Jin H, Wang M, Zhang Y, et al. Deletion of the transforming growth factor  $\beta$  receptor type II gene in articular chondrocytes leads to a progressive osteoarthritis-like phenotype in mice. *Arthritis Rheum* 2013;65(12):3107-19.
55. Davidson EB, Van der Kraan P, Van Den Berg W. TGF- $\beta$  and osteoarthritis. *Osteoarthr. Cartil* 2007;15(6):597-604.
56. Yu F-F, Zuo J, Fu X, Gao M-H, Sun L, Yu S-Y, et al. Role of the hippo signaling pathway in the extracellular matrix degradation of chondrocytes induced by fluoride exposure. *Ecotoxicol Environ Saf* 2021;225:112796.
57. Finsson K, Parker W, Chi Y, Hoemann C, Goldring M, Antoniou J, et al. Endoglin differentially regulates TGF- $\beta$ -induced Smad2/3 and Smad1/5 signalling and its expression correlates with extracellular matrix production and cellular differentiation state in human chondrocytes. *Osteoarthr. Cartil* 2010;18(11):1518-27.
58. McLean S, Di Guglielmo GM. TGF $\beta$  (transforming growth factor  $\beta$ ) receptor type III directs clathrin-mediated endocytosis of TGF $\beta$  receptor types I and II. *Biochem J* 2010;429(1):137-45.
59. Akasaki Y, Hasegawa A, Saito M, Asahara H, Iwamoto Y, Lotz M. Dysregulated FOXO transcription factors in articular cartilage in aging and osteoarthritis. *Osteoarthr. Cartil* 2014;22(1):162-70.
60. Shen C, Cai G-Q, Peng J-P, Chen X-D. Autophagy protects chondrocytes from glucocorticoids-induced apoptosis via ROS/Akt/FOXO3 signaling. *Osteoarthr. Cartil* 2015;23(12):2279-87.
61. Eelen G, Verlinden L, Maes C, Beullens I, Gysemans C, Paik J-H, et al. Forkhead box O transcription factors in chondrocytes regulate endochondral bone formation. *J Steroid Biochem Mol Biol* 2016;164:337-43.
62. Kao W-C, Chen J-C, Liu P-C, Lu C-C, Lin S-Y, Chuang S-C, et al. The Role of Autophagy in Osteoarthritic Cartilage. *Biomolecules* 2022;12(10):1357.
63. Gholipour A, Malakootian M, Oveisee M. hsa-miR-508-5p as a New Potential Player in Intervertebral Disc Degeneration. *IJM-CM* 2022; 11(2): 137-149.
64. Liu S, Cao C, Zhang Y, Liu G, Ren W, Ye Y, et al. PI3K/Akt inhibitor partly decreases TNF- $\alpha$ -induced activation of fibroblast-like synoviocytes in osteoarthritis. *J Orthop Surg Res* 2019;14(1):1-13.
65. Montaseri A, Busch F, Mobasheri A, Buhmann C, Aldinger C, Rad JS, et al. IGF-1 and PDGF-bb suppress IL-1 $\beta$ -induced cartilage degradation through down-regulation of NF- $\kappa$ B signaling: involvement of Src/PI-3K/AKT pathway. *PLoS one* 2011;6(12):e28663.
66. Litherland GJ, Dixon C, Lakey RL, Robson T, Jones D, Young DA, et al. Synergistic collagenase expression and cartilage collagenolysis are phosphatidylinositol 3-kinase/Akt signaling-dependent. *J Biol Chem* 2008;283(21):14221-9.
67. Zhang Y, Vasheghani F, Li Y-h, Blati M, Simeone K, Fahmi H, et al. Cartilage-specific deletion of mTOR upregulates autophagy and protects mice from osteoarthritis. *ARD* 2015;74(7):1432-40.
68. Malakootian M, Gholipour A, Oveisee M. CD19, ALDH18A1, and CACNA1G as Significant Hub Genes in End-Stage Osteoarthritis. *IJPH* 2023;52(12):2651-62.